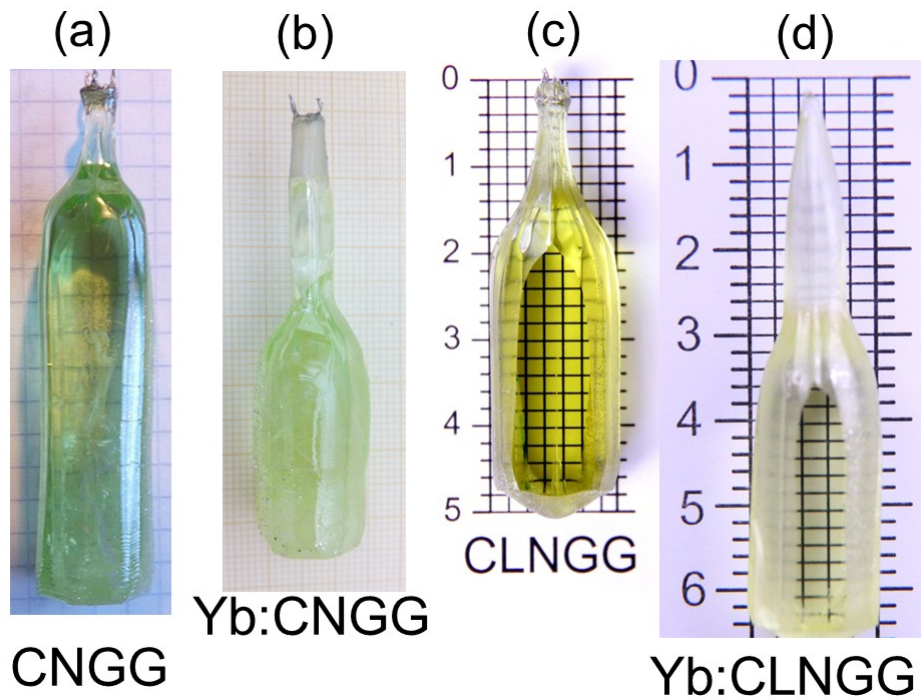


**Design of Yb<sup>3+</sup> optical bandwidths by crystallographic modification of  
disordered Calcium Niobium Gallium laser garnets**

M. D. Serrano, J. O. Álvarez-Pérez, C. Zaldo, J. Sanz, I. Sobrados, J. A. Alonso, C. Cascales\*, M. T. Fernández-Díaz and A. Jezowski

**ELECTRONIC SUPPLEMENTARY INFORMATION**

## CZOCHELSKI GROWTH OF $\text{CaNbGa}$ GARNET CRYSTALS



**Figure ESI.1.** Single crystals grown by the Czochralski method. (a) Undoped CNGG, (b) 11.6at% Yb:CNGG, (c) undoped CLNGG (2 parallel sides polished), crystal grown with 99.5% purity  $\text{CaCO}_3$ , and (d) 8at% Yb:CLNGG (2 parallel sides polished), crystal grown with 99.99% purity  $\text{CaCO}_3$ . The scale in the figures is in centimeters.

## CRYSTALLOGRAPHIC INFORMATION

**Table ESI.1** Structure refinement details and crystal data at 296±2 K for CLNGG and 8at% Yb:CLNGG crystals by using single crystal X-ray diffraction data.

	CLNGG <sup>a</sup>	8at% Yb:CLNGG <sup>b</sup>
Wavelength (Å)	0.71073	
Crystal system, space group, Z	Cubic, <i>Ia-3d</i> (No. 230), 8	
Unit cell dimension (Å), Volume (Å <sup>3</sup> )	12.5064(1), 1956.13(3)	12.4825(1), 1944.93(3)
Calculated density (Mg/m <sup>3</sup> )	4.657	4.911
Absorption coefficient (mm <sup>-1</sup> )	11.794	14.105
Crystal size (mm <sup>3</sup> )	0.40 × 0.10 × 0.12	0.03 × 0.10 × 0.11
θ range for data collection (deg)	3.99 to 30.44	4.00 to 36.38
Limiting indices	-17≤h≤17, -17≤k≤17, -17≤l≤17	-20≤h≤20, -17≤k≤20, 18≤l≤20
Reflections collected	39726	25183
Independent reflections	254 [R(int) = 0.0428]	404 [R(int) = 0.0489]
Completeness to θ, %	30.44, 100	36.38, 100
Absorption correction	Multi-scan SADABS	
Refinement method	Full-matrix least squares on F <sup>2</sup>	
Goodness-of-fit on F2	1.141	1.140
R indices [I>2σ(I)], R1,	0.0116	0.0142
wR2	0.0221	0.0271
R indices (all data), R1	0.0135	0.0209
wR2	0.0222	0.0290
Extinction coefficient	0.00143(4)	0.00269(7)
Largest diff. peak and hole (eÅ <sup>-3</sup> )	0.260 and -0.258	0.346 and -0.362

<sup>a</sup>The total exposure time for data collection was 5.65 h. The frames were integrated with the Bruker SAINT software package using a narrow-frame algorithm. The starting cell constant *a* is derived upon the refinement of the XYZ-centroids of 7108 reflections I> 20 σ(I) with 7.982 deg < 2θ < 60.25 deg.

<sup>b</sup>The total exposure time for data collection was 3.01 h. The frames were integrated with the Bruker SAINT software package using a narrow-frame algorithm. The starting cell constant *a* is derived upon the refinement of the XYZ-centroids of 4098 reflections I> 20 σ(I) with 7.997 deg < 2θ < 70.20 deg.

**Table ESI.2** Atomic coordinates (×10<sup>4</sup>), occupancy factor, OF, and equivalent isotropic displacement parameters U(eq) (Å<sup>2</sup>×10<sup>3</sup>) for CLNGG and 8at% Yb:CLNGG crystals from scXRD data. U(eq) is defined as one third of the trace of the orthogonalized U<sub>ij</sub> tensor. Note that atomic coordinates for O atoms are given with one order lower accuracy than those obtained from pND data (Table 2 in the main text).

Ion	site	CLNGG					8at% Yb:CLNGG				
		<i>x</i>	<i>y</i>	<i>z</i>	OF	U(eq)	<i>x</i>	<i>y</i>	<i>z</i>	OF	U(eq)
Ca	24 <i>c</i>	0	2500	1250	0.986(6)	9(1)	0	2500	1250	0.937(1)	8(1)
Yb	24 <i>c</i>	-	-	-	-	-	0	2500	1250	0.063(1)	8(1)
Nb(1)	16 <i>a</i>	0	0	0	0.66(3)	6(1)	0	0	0	0.67(3)	5(1)
Ga(1)	16 <i>a</i>	0	0	0	0.34(4)	6(1)	0	0	0	0.35(3)	5(1)
Ga(2)	24 <i>d</i>	0	2500	8750	0.81(4)	6(1)	0	2500	8750	0.772(4)	6(1)
Nb(2)	24 <i>d</i>	0	2500	8750	0.05(4)	6(1)	0	2500	8750	0.088(4)	6(1)
O	96 <i>h</i>	506(1)	1475(1)	9695(1)		9(1)	510(1)	1478(1)	9696(1)		8(1)

## HYPOTHETICAL STRUCTURAL MODELS FOR Li DISTRIBUTION IN THE CNGG-TYPE GARNET STRUCTURE: RESULTS OF CORRESPONDING PRELIMINARY SINGLE CRYSTAL XRD REFINEMENTS FOR THE CLNGG CRYSTAL

Taking into account the used amounts of reagents for preparing the CLNGG crystal (before the synthesis of the garnet phase, see the main text), 0.275 of Li per CLNGG formula will be considered as the starting quantity of Li in next structural refinements. Since unfortunately the neutron bound coherent scattering lengths (in fm) of Nb and Ga are very similar, 7.054 and 7.288 respectively, and thus any reliable refinement of their relative populations over a same crystal site is hampered using neutron diffraction data, different models for Li distribution in the CNGG-type garnet structure were preliminarily evaluated by refinements using single crystal XRD data with the SHELXTL program.

Three hypothetical structure models were considered: A) Li located only in octahedral 16*a* sites, B) Li located in both octahedral 16*a* and tetrahedral 24*d* sites, and C) Li located only in tetrahedral 24*d* sites.

In A and B models the starting population factors of Li in 16*a* sites were 0.1375 and 0.0688, respectively, with a further Li starting population factor of 0.0458 in 24*d* for B model (i.e. 50% of “nominal” Li in each kind of site). If no restraint over the population of 16*a* sites is applied (to test if 16*a* sites are fully occupied by Nb, Ga and Li cations or if there are vacancies), the refinements were unstable and they do not converge. On the other hand, when the restraint over the population of 16*a* is imposed (i.e. the site 16*a* is considered to be fully occupied by Nb, Ga and Li, with no octahedral vacancies), the refinement of the A model yields cationic populations of Nb  $0.63 \pm 0.03$ , Ga  $0.39 \pm 0.04$  and Li  $-0.02 \pm 0.01$  over 16*a* sites, with  $R_1 = 0.0117$ , being the populations of Ca over dodecahedral 24*c*, and of Ga and Nb over tetrahedral 24*d* almost the same that those in the scXRD refinement previously reported (with results in Table ESI.2). The slightly negative Li population obtained from refinement of the A model indicates that Li is not located in octahedral 16*a* sites, and in fact after removing Li of 16*a* sites, the refinement converges to the Table ESI.2 population values over 24*c*, 16*a* and 24*d* sites, with about 14% of vacancies over tetrahedral 24*d* sites. In the refinement of the B model with 16*a* sites restrained to be fully occupied, after some cycles that yield populations of Nb  $0.59 \pm 0.20$ , Ga  $0.43 \pm 0.23$  and Li  $-0.03 \pm 0.06$  over 16*a* sites, the refinement became unstable and it does not converge.

On the other hand, any scXRD refinement with all “nominal” Li only in tetrahedral 24*d* sites, the C model, has no physical meaning since previous (E. Castellano-Hernández et al., *Cryst. Growth Des.* 2016, 16, 1480) and current refinements of CNGG-type garnets reveal the existence of an important level of vacancies in these 24*d* sites, indistinguishable of Li in scXRD refinements.

A more realistic approach for analyzing A, B and C hypothetical structure models was based on the analysis of vacancies over 16*a* and 24*d* sites, in such a way that if the

refinement yields vacancies, these latter should be an indication of the possible Li presence in these sites.

Considering again the model A, only Nb and Ga were located in  $16a$  sites, and no restraint is applied over the population of these sites. The resulting  $16a$  populations were Nb  $0.65\pm 0.04$  and Ga  $0.36\pm 0.04$ , and  $R_1 = 0.0119$ , with populations of Ca over dodecahedral  $24c$  and Ga and Nb (and vacancies) over tetrahedral  $24d$  sites nearly the same as in Table ESI.2. Results of the refinement indicate, once again, that the octahedral  $16a$  sites are fully occupied by Nb and Ga, with no vacancies, thus no Li is located in  $16a$  sites.

In the model B, with Nb and Ga located in  $16a$  and in  $24d$  sites, and no restraints applied over the population of both kinds of sites, the refinement yielded population factors of Nb  $0.62\pm 0.03$  and Ga  $0.40\pm 0.04$  in  $16a$  sites, and Ga  $0.83\pm 0.04$  and Nb  $0.04\pm 0.04$  in  $24d$  sites,  $R_1 = 0.0116$ , that is, a full Nb+Ga occupation of octahedral  $16a$  sites, thus excluding the location of Li in these sites, while up to 13% of vacancies over tetrahedral sites are disclosed. Some of these vacancies may correspond to Li cations in these  $24d$  positions, thus it seems clear that the only possibility for Li location is that of model C, which has been then tested with pND data, as indicated in the main text.

In summary, every of the attempted scXRD refinements to locate Li has provided the same clear indication about the CLNGG crystal structure: the  $16a$  octahedral positions are fully occupied by Nb and Ga, in a ratio of about 2:1, and only about 87% of  $24d$  tetrahedral sites are occupied by Ga (predominantly) and by Nb (a very small amount) being the remaining 13% either vacant or occupied by Li, as it has been tested and demonstrated by the current refinement using pND data presented in the main text.

## OPTICAL PROPERTIES

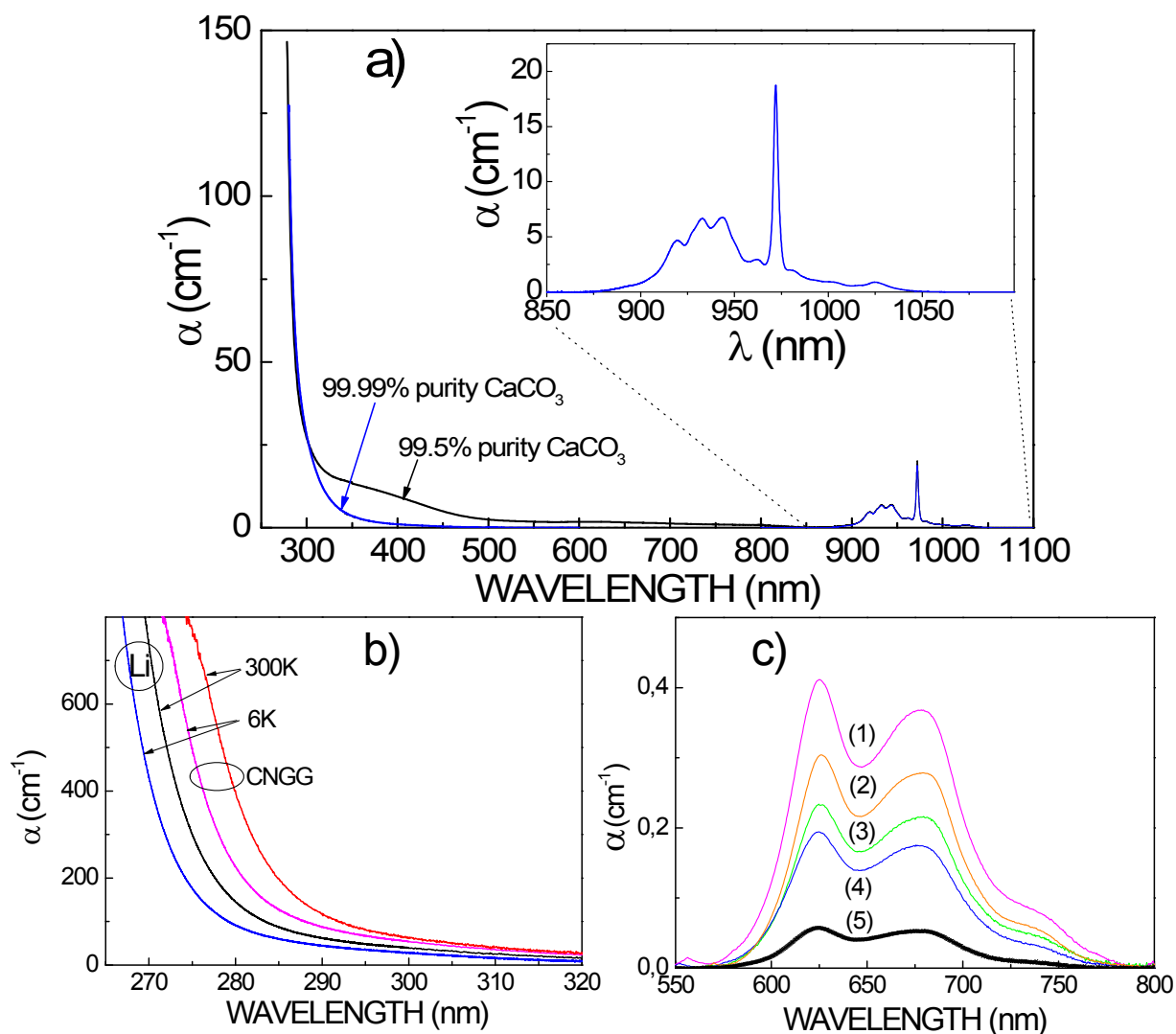


**Figure ESI.2** a) General view of the RT optical absorption of 8at% Yb:CLNGG prepared with 99.5% purity  $\text{CaCO}_3$  (black line) showing the bandgap absorption in the ultraviolet ( $\lambda < 290$  nm), a broad pre-edge absorption from  $\lambda = 500$  nm to the absorption bandgap edge, absorption bands associated with crystal coloration ( $\lambda = 570$ -800 nm) and  $\text{Yb}^{3+}$  absorption ( $\lambda = 850$ -1050 nm). The 8at%Yb:CLNGG crystal grown with 99.99%  $\text{CaCO}_3$  (blue line) is free of pre-edge absorption. b) Detailed comparison of the ultraviolet absorption edge of undoped CLNGG (40  $\mu\text{m}$  thick plate) and CNGG (68  $\mu\text{m}$  thick plate) crystals: at 300 K, CLNGG (black line), CNGG (red line), and at 6 K, CLNGG (blue line), CNGG (magenta line). (c) RT optical absorption of CNGG-type crystals leading to greenish coloration: (1) 8at%Yb:CMNGG modified with extra 7.5% (with respect to Nb) of Mg. (2) 0.3at%Yb:CNGG. (3) Undoped CLNGG. (4) 8 at% Yb:CLNGG grown with 99.5%  $\text{CaCO}_3$ . (5) 8 at% Yb:CLNGG grown with 99.99%  $\text{CaCO}_3$ .

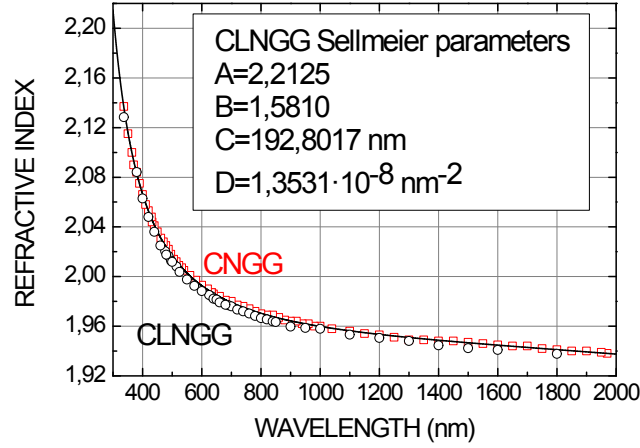


**Figure ESI.3** Refractive index dispersion,  $n(\lambda)$ , of undoped CLNGG single crystal ( $\circ$ ) and its fit (continuous line) to the Sellmeier law with the parameter set given in the inset. For comparison  $n(\lambda)$  of undoped CNGG single crystal ( $\square$ ) has been also included.

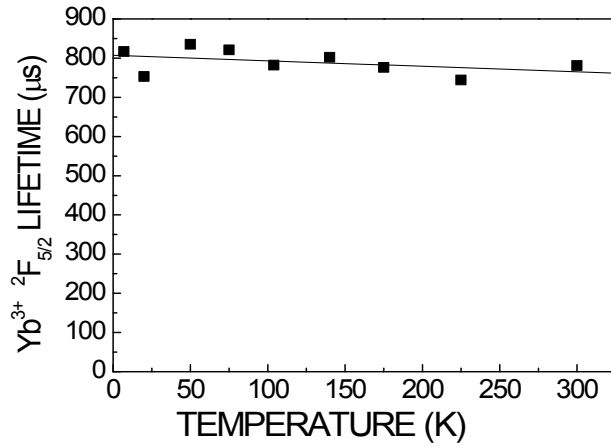


**Figure ESI.4** Thermal evolution of the  ${}^2F_{5/2}$  fluorescence lifetime of  $\text{Yb}^{3+}$  in the 0.3at% Yb:CNGG crystal,  $\lambda_{\text{EXC}}=971$  nm,  $\lambda_{\text{EMI}}=1021$  nm.

## CRYSTAL FIELD SIMULATIONS

In the Simple Overlap Model (SOM) the crystal field parameters (CFPs) are calculated from the atomic positions in the structure. It is assumed that the interaction energy of trivalent lanthanide  $\text{Ln}^{3+}$  in a chemical environment is produced by an electrostatic potential of charges uniformly distributed over small regions centered around the midpoint of the  $R_L$  distance from  $\text{Ln}^{3+}$  to the ligand L,  $R_0$  being the shortest distance. The charge in each region is proportional to the total overlap integral  $\rho$  between the 4f and the s and p orbitals of the  $\text{Ln}^{3+}$  and L, respectively. The CFPs are written as

$$B_q^k = \langle r^k \rangle \sum_L \rho_\mu \left( \frac{2}{1 \pm \rho_L} \right)^{k+1} A_q^k(L), \quad \rho_L = \rho_0 \left( \frac{R_0}{R_L} \right)^{3.5} \quad [1].$$

The sum over L is restricted to the first neighbors, i.e. over all ligands of the first coordination sphere, consequently the required crystallographic data are restricted to the closest ligand positions and thus  $\langle r^k \rangle$  radial integrals are not corrected from the spatial expansion.  $A_q^k$  is the lattice sum and it takes into account the symmetry properties of the  $\text{Ln}^{3+}$  site, including the effective charge attributed to L. The sign  $\pm$  of the denominator stands for differentiating the type of L: when a single type of L is considered, a minus sign corresponding to the normal shift of the charge barycenter from the mid-point of the  $R_L$  bonding distance should be taken, and when different L are present the minus sign corresponds to the most covalent one.

The SOMPLUS model, an extension of SOM, allows estimating CFPs from the crystallographic positions and distances of all atoms, oxygens and first sphere of nearest cations, around the central  $\text{Ln}^{3+}$ . Effects from different cations at a same crystal site arise by considering individual effective charges. Charge compensation and vacancies at a given site can be also taken into account in the SOMPLUS model.

**Table ESI.3** Effect of the substitution of one tetrahedral  $24d$   $\text{Ga}^{3+}$  (at 3.12 Å) on the crystal field potential of  $24c$   $\text{Yb}^{3+}$  in disordered  $\text{CaNbGa}$  garnets: SOMPLUS calculated crystal field parameters ( $\text{cm}^{-1}$ ). Effective charges: 0.2, 0.6, 1.4, 2.4, and 3.7 for  $\text{Li}^+$ ,  $\text{Mg}^{2+}$ ,  $\text{Ga}^{3+}$ ,  $\text{Ge}^{4+}$  and  $\text{Nb}^{5+}$ , respectively, and  $\rho=0.8$ .

	$1\Box_{\text{T}}$	$1\text{Li}_{\text{T}}^+$	$1\text{Mg}_{\text{T}}^{2+}$	$1\text{Ga}_{\text{T}}^{3+}$	$1\text{Ge}_{\text{T}}^{4+}$	$1\text{Nb}_{\text{T}}^{5+}$
$B_0^2$	-646	-629	-597	-531	-450	-344
$B_2^2$	614	595	555	476	379	255
$B_0^4$	615	613	608	599	588	573
$B_2^4$	411	413	417	424	430	427
$B_4^4$	40	38	31	18	1	-18
$B_0^6$	694	695	696	699	703	707
$B_2^6$	-458	-458	-459	-460	-458	-444
$B_4^6$	45	46	47	49	51	47
$B_6^6$	-612	-610	-599	-577	-515	-310
$iB_2^4$	71	73	80	92	117	175
$iB_4^4$	28	27	26	23	17	3
$iB_2^6$	-72	-73	-80	-92	-116	-175
$iB_4^6$	45	11	13	17	24	39
$iB_6^6$	-297	-305	-331	-376	-465	-629

By using SOMPLUS, CFPs calculations for  $24c$   $\text{Yb}^{3+}$  in disordered  $\text{CaNbGa}$  garnets take into account the effect from nearest  $24d$  sites when one  $\text{Ga}^{3+}$  (at 3.12 Å from central  $24c$   $\text{Yb}^{3+}$ ) is replaced by one vacancy  $\Box_{\text{T}}$ , or by one  $\text{Li}^+$ ,  $\text{Mg}^{2+}$ ,  $\text{Ge}^{4+}$  or  $\text{Nb}^{5+}$  cation. Table ESI.3 gives derived CFPs (real  $B_q^k$  and complex  $iB_q^k$ ) in each case, which

correspond to a local symmetry lower than the  $D_2$  symmetry of the  $\text{YbO}_8$  dodecahedron in the garnet.

### $\text{Yb}^{3+}$ SPECTROSCOPY

Figure ESI.5 shows the decomposition of the 0-0'  $\text{Yb}^{3+}$  6 K OA in Mg-modified 8at%Yb:CMNGG crystal by following the procedures described in the Discussion section of the main text, with the following  $I_0$ ,  $E_0$ ,  $\omega$  parameters:

$\text{Ga}^{3+}-\square_{\text{T}}^0$	0.055, 10276.8, 5.5
$\text{Ga}^{3+}-\text{Mg}^{2+}$	0.128, 10290.2, 2.9, +0.018, 10283.5, 2.7, +0.013, 10274.3, 2.0
$\text{Ga}^{3+}-\text{Ga}^{3+}$	0.491, 10299.87, 4.8, +0.154, 10293.2, 4.8, +0.053, 10284, 3.5
$\text{Ga}^{3+}-\text{Nb}^{5+}$	0.035, 10312, 2.5

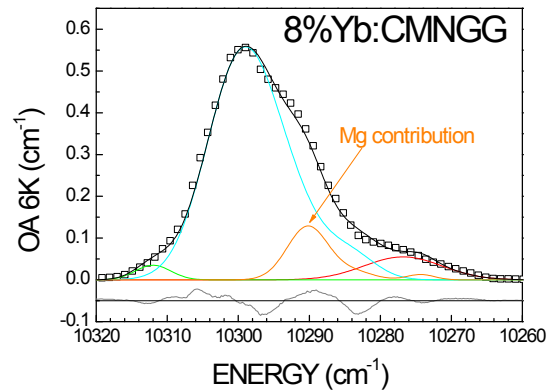


**Figure ESI.5** Fit of the 6 K 0-0' Yb OA of a 8at%Yb:CMNGG crystal (30at% extra Mg with respect to Nb).  $\square_{\text{T}}$ , experimental results. Red, orange, blue and green lines are the contributions of the nearest tetrahedra (3.12 Å) to central  $\text{Yb}^{3+}$  occupied by vacancy  $\square_{\text{T}}$ ,  $\text{Mg}^{2+}$ ,  $\text{Ga}^{3+}$  or  $\text{Nb}^{5+}$ , respectively. The black line is the fit and the bottom gray line is the fit error.

**Table ESI.4** Probabilities P of Ga, Nb, vacancy ( $\square_{\text{T}}$ ), and Li cationic distributions on the two (n=2) edge sharing nearest neighbors at 3.12Å 24d tetrahedral sites around a dodecahedral 24c  $\text{Yb}^{3+}$  site in 0.3at%Yb:CNGG and 8at% Yb:CLNGG crystals.

0.3at%Yb:CNGG		8at%Yb:CLNGG	
Ga:Nb: $\square_{\text{T}}$	P	Ga:Nb:Li	P
2:0:0	0.674	2:0:0	0.656
1:1:0	0.166	1:0:1	0.178
1:0:1	0.126	1:1:0	0.113
0:1:1	0.016	0:0:2	0.024
0:2:0	0.010	0:1:1	0.015
0:0:2	0.006	0:2:0	0.005

Table ESI.4 gives the probabilities  $P$  calculated according the description made in the main text of the more likely sharing edges tetrahedral cationic distributions around  $24c$   $\text{Yb}^{3+}$  for  $0.3\text{at}\%\text{Yb}:\text{CNGG}$  and  $8\text{at}\%\text{Yb}:\text{CLNGG}$  crystals, using OF given in Table 4. From Table ESI.4 it is obvious that the most probable cationic configuration over the edge sharing tetrahedra, i.e.  $\text{Ga}^{3+}-\text{Ga}^{3+}$ , is much more probable than the two next  $\text{Ga}^{3+}-\text{Nb}^{5+}$  or  $\text{Ga}^{3+}-\square_{\text{T}}$ , being probability of the rest one order of magnitude lower than the latter. Consequently, a large band and two minor ones are expected, that agrees the experimental result shown in Figure 13a.

Figure ESI.6 shows the 300 K photoluminescence emission spectra of  $8\text{at}\%\text{Yb}:\text{CNGG}$  and  $8\text{at}\%\text{Yb}:\text{CLNGG}$  under excitation at different wavelengths inside the OA of  $\text{Yb}^{3+}$ . It is worth noting that the shape of the luminescence spectra is insensitive to the excitation wavelength. This corresponds to strong Yb-Yb energy transfer and thus the excitation of all coexisting Yb centers.

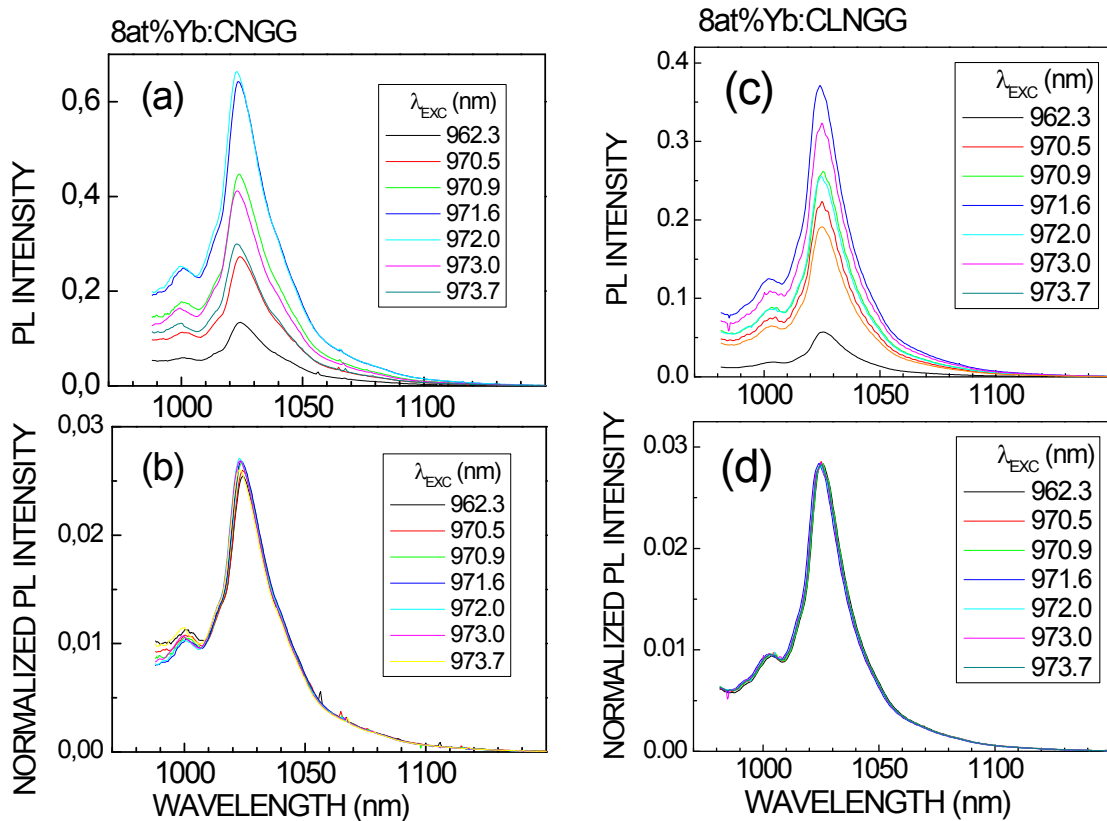


**Figure ESI.6** 300 K luminescence spectra of  $\text{Yb}^{3+}$  in CNGG-type crystals for different excitation wavelengths. (a,b)  $8\text{at}\%\text{Yb}:\text{CNGG}$ . (c,d)  $8\text{at}\%\text{Yb}:\text{CLNGG}$ . In the bottom row (b and d) the luminescence intensity was normalized to the integrated area.